J Mater Sci (2010) 45:2930–2937
DOI 10.1007/s10853-010-4285-y

Thermal characteristics and crystallization kinetics of tellurite glass with small amount of additive As_2O_3

E. Yousef · A. El-Adawy · M. H. Makled · A. E. Al-Salami

Received: 28 October 2009 / Accepted: 28 January 2010 / Published online: 9 March 2010

Abstract The crystallization kinetics of the $TeO_2/TiO_2/As_2O_3$ glassy system was studied under nonisothermal conditions. The method was applied to the experimental data obtained by differential thermal analysis (DTA), using continuous-heating techniques. In addition, two approaches were used to analyze the dependence of glass transition temperature (T_g) on the heating rate (β): One is the empirical linear relationship between (T_g) and (β); The other approach is the use of straight line from the plot of $\ln\left(T_g^2/\beta\right)$ vs. $1/T_g$ for evaluation of the activation energy for glass transition. The crystallization results are analyzed, and both the activation energy of crystallization process and the crystallization mechanism are characterized.

Introduction

In the last two decades, tellurite glasses have attracted a great deal of interest due to their high refractive index, and high phonon energy which enlarges the transmission infrared spectra range up to ≅6 μm [1–3]. Tellurite glasses have been considered as promising materials for both fiber amplifiers and nonlinear optical devices [4]. These properties, due to high polarizability of Te^{4+} ions (with a solitary electron pair $5s^2$) can be even more enhanced by means of the incorporation of other heavy metal oxides that can be easily polarized (e.g., those of sixth period, like Tl^+, Bi^{3+}, Pb^{2+}) or with empty d orbital (e.g., W^{6+}, Zr^{4+}, Ti^{4+}, and Nb^{5+}) [5]. Three structural entities of TeO_2 have been reported [6] as follows: (1) TeO_4 trigonal bipyramids (tbp) group with two axial and equatorial oxygen atoms; (2) TeO_{3+1} asymmetric polyhedron in which one Te–O axial bond shortens while the other elongates; and (3) TeO_3 trigonal pyramids (tp) with three short Te–O distances. Among the modifiers TiO_2 is of special interest. Moreover, the recent ab initio studies of $[TeO_2]_p$ clusters provide arguments to associate the above mentioned extraordinary optic properties with the essential nonlocality of the electron dielectric response, which is found to be characteristic of the $[TeO_2]_p$ chainlike polymers [7]. Actually, the X-ray diffraction patterns and the Raman spectra show that no $[TeO_3]^{2-}$ pyramids and thus no $[Te_pO_q]^{-2(q-2p)-}$ anions appear in crystalline or glassy structures within the TeO_2–TiO_2 system [8] which would keep the framework nature of such compounds, thus favoring their high polarizability and hyperpolarizability. Other advantages of such glasses are their good thermal and chemical stabilities, low tendency to crystallization, and their ability to host rare earth ions [2]. When As_2O_3 is present in TeO_2 glass network, it is quite possible for a cross linking of a part of TeO_4 units to combine with As_2O_3 unit to form As–O–Te bonds in the glass network [9]. Earlier, arsenic oxide was being used as a fining agent to remove air bubbles in the glasses [10]. Chung and Mackenzie [11] have suggested that a small

E. Yousef (✉)
Faculty of Science, Physics Department, Al Azhar University, Assuit Branch, Assuit, Egypt
e-mail: omn_yousef2000@yahoo.com

A. El-Adawy
Faculty of Science, Physics Department, Monofia University, Shebin Elkom, Monofia, Egypt
e-mail: amin_el_adawy@hotmail.com

M. H. Makled
Faculty of Science, Physics Department, Benha University, Benha, Alkloubia, Egypt

Present Address:
E. Yousef · A. E. Al-Salami
Faculty of Science, Physics Department, King Khalid University, P.O. Box 9003, Abha, Saudi Arabia

number of V^{4+} ions would be reduced to V^{3+} state, as per the following equation:

$$As_2O_3 + V_2O_5 \rightarrow As_2O_5 + V_2O_3;$$

Therefore, we can suggest that, during the melting of the present glasses at higher temperature, there is a possibility that the following redox equilibrium takes place: $As_2O_3 + TeO_2 \rightarrow Te^0 + As_2O_5$. The aim of this article is to evaluate the activation energy for glass transition and crystallization for these glasses.

Theoretical background

The formal theory of transformation kinetics is the one was developed by Avrami [12]. This theory supposes that the crystal growth rate in general is anisotropic, and in the case of an as quenched glass where a large number of nuclei already exists and no new nuclei are formed during thermal treatment, the volume fraction crystallized, χ, is expressed in terms of the crystal growth, u, as function on time (t) is as follows:

$$\chi = 1 - \exp\left[\left(-g\int_0^t u(t')\mathrm{d}t'\right)^m\right] \tag{1}$$

where g is a geometric factor and, m, is an exponent related to the dimensionality of the crystal growth. In the considered case (i.e., site saturation) [13] the kinetic exponent is $n = m$, and assuming an Arrhenian temperature dependence for, u [14], and a constant heating rate $\beta = \mathrm{d}T/\mathrm{d}t$, the extended volume fraction, χ_e, becomes

$$\chi_e = gN_0\left(\frac{u_0}{\beta}\right)^n\left(\int_{T_0}^{T} e^{-E_G/RT'}\mathrm{d}T'\right)^n = QI^n \tag{2}$$

where, T_0 is the initial temperature of the non-isothermal process, E_G is the effective activation energy for crystal growth, and N_0 is the number of pre-existing nuclei per unit volume. Substituting for $z' = E_G/RT'$, the integral, I, can be represented by an alternating series where it is possible to use only first term without making any appreciable error, and by assuming that $T_0 \ll T$ [15, 16] we obtain I

$$I = \frac{RT^2}{E_G}\exp\left(-\frac{E_G}{RT}\right) \tag{3}$$

Substituting Eq. 3 into Eq. 2, introducing the parameter, $L = (R/E_G)^n$, and defining the reaction rate constant as $K_v = (gN_0)^{1/n}u_0\exp(-E_G/RT)$, with an Arrhenian temperature dependence, the volume fraction crystallized is expressed as

$$\chi_e = L\left(K_vT^2\beta^{-1}\right)^n \tag{4}$$

The relation between the actual fraction, χ, and the extended, χ_e, can be written as [17]

$$\mathrm{d}\chi = (1-\chi)\mathrm{d}\chi_e \tag{5}$$

and so the Eq. 4 can be rewritten as follows:

$$\chi = 1 - \exp\left[-L\left(K_vT^2\beta^{-1}\right)^n\right] \tag{6}$$

Differentiating Eq. 6 with respect to time, the crystallization rate is obtained as

$$\frac{\mathrm{d}\chi}{\mathrm{d}t} = nL(1-\chi)\left(K_vE_GR^{-1} + 2K_vT\right)\left(\frac{K_vT^2}{\beta}\right)^{n-1} \tag{7}$$

The maximum crystallization rate is found by making $\frac{\mathrm{d}^2\chi}{\mathrm{d}t^2} = 0$, and thus obtaining the relationship from Eq. 7 as follows [18]:

$$\begin{aligned} Y_b &= -\ln(1-\chi_P) = L\left(\frac{K_vT_P^2}{\beta}\right)^n, \\ &= 1 - \frac{2}{n}\left(1 + \frac{E_G}{RT_P}\right)\left(2 + \frac{E_G}{RT_P}\right)^{-2}, \end{aligned} \tag{8}$$

where the subscript, P, denotes the magnitude values corresponding to the maximum crystallization rate. In most crystallization reactions, $\frac{E_G}{RT_P} \succ\succ 1$, and the logarithmic form of Eq. 8 is written as

$$\ln\left(\frac{T_P^2}{\beta}\right) = \frac{E_G}{RT_P} - \ln\left(L^{1/n}K_v\right) \tag{9}$$

From the linear relationship of Eq. 9, it is possible to calculate the kinetic parameters E_G and L. At the same time, if the expression $L^{1/n}(K_v)_PT_P^2/\beta = 1$ is introduced into Eq. 7, then one obtains

$$n = \left(\frac{\mathrm{d}\chi}{\mathrm{d}t}\right)_P RT_P^2(0.37\beta E_G)^{-1} \tag{10}$$

which makes it possible to calculate the kinetic exponent, n.

Experimental details

The glass systems $TeO_2/(1-x)$ $TiO_2/0.03$ mol% As_2O_3 where ($x = 0.06$, 0.12, and 0.15 mol%), were prepared by mixing specified weights of tellurium oxide (TeO_2, 99.9% purity, Ferak), Titanium oxide (TiO_2, 99.99% purity, Sigma-Aldrich), and Arsenic oxide (As_2O_3, 99.9% purity, Aldrich). The powder mixture was heated in a platinum crucible at 773 K for 30 min to avoid the volatilization of Arsenic oxide and then heated in a melting furnace to a temperature of 1173 K for 30 min. The melt which had a high viscosity was cast in a brass mold. Subsequently, the sample was transferred to an annealing furnace and kept for

2 h at 600 K. Then, the furnace was switched off, and the glass sample was allowed to cool, and the glass formed was homogenous. The color of these samples is pale yellow, and it is transparent.

The thermal behavior was investigated using differential thermal analysis (Shimadzu DTA 50) to determine glass transition temperature T_g (in K), initial crystallization temperature T_0 (in K), and the peak temperature of crystallization T_P (in K). The temperature and energy calibrations of the instrument were performed using the well-known melting temperature and the melting enthalpy of high purity indium metal. The thermal sensitivity is 10 μv, and the temperature precision is ±1.0 K. The crystallization thermogram was increased at a uniform rate β ranging from 5 to 20 K min^{-1}.

Result and discussion

The thermal characteristics of the prepared glasses are given in Table 1 and Fig. 1. The prepared glasses exhibit endothermic effects due to glass transition temperature (T_g) ranging between 620 and 639 K at the rate of 10 K min^{-1}. It is found that the T_g value increases with increasing concentration of TiO_2 content, thereby indicating the substitution of the Te–O–Te bridges inherent of pure TeO_2 by the stronger chemical linkage Te–O–Ti. The appearance of a single peak due to the glass transition temperature in DTA pattern of all the prepared glasses indicates existence of the high homogeneity in the glass matrix. The thermal stability of the glasses was calculated as the difference between the onset crystallization temperature (T_0) and the glass transition temperature (T_g) $\left(\Delta T = T_0 - T_g \text{ in } K\right)$.

Two approaches are used for the analysis of the dependence of T_g on the heating rate. The first is the

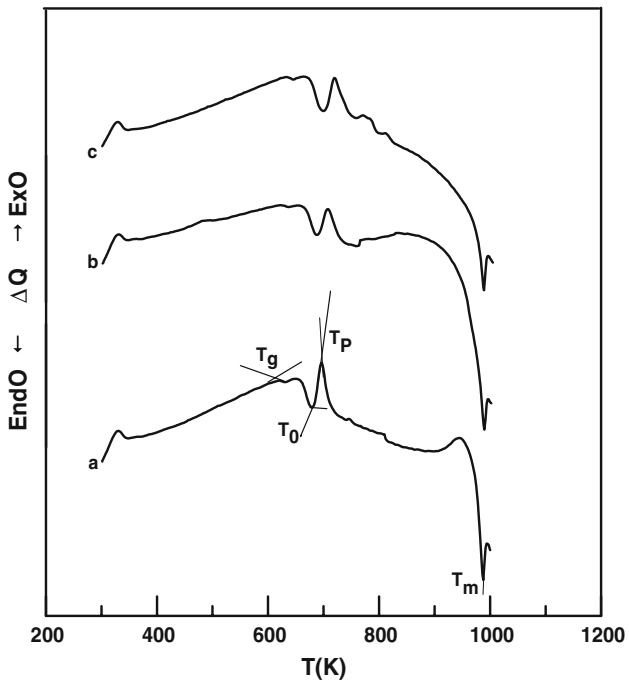

Fig. 1 DTA traces for prepared glasses at heating rate 10 K min^{-1}. (*a*) sample 1, (*b*) sample 2, and (*c*) sample 3

empirical relation that has been suggested by Lasoka [19] and has the form:

$$T_g = A + B \ln \beta \tag{11}$$

where A and B are constants. The plots of T_g versus ln β for all the glasses are shown in Fig. 2. From the linear regression, values of A and B are obtained. They are summarized in Table 2—columns 2 and 3. The value of A indicates the glass temperature for the heating rate of 1.0 K min^{-1}. It has been found by the various researchers

Table 1 Crystallization rate β, glass transition T_g, onset crystallization temperature T_0, thermal stability temperature ΔT, exothermic peak of crystallization T_p, kinetic exponent and average of kinetic exponent <*n*> of studied glasses

Sample name	System composition in mol%			Rate β in K min^{-1}	T_g In K	T_0 In K	ΔT In K	T_p In K	*n*	<*n*>
Sample 1	$0.94TeO_2$	$0.06TiO_2$	$0.03As_2O_3$	5	614	668	54	681	0.77	1.07
				10	620	674	54	689	1.25	
				15	626	677	51	693	1.15	
				20	630	682	52	696	1.11	
Sample 2	$0.88TeO_2$	$0.12TiO_2$	$0.03As_2O_3$	5	623	675	52	691	0.6	0.845
				10	629	682	53	700	0.9	
				15	633	686	53	705	0.9	
				20	638	690	52	708	0.98	
Sample 3	$0.85TeO_2$	$0.15TiO_2$	$0.03As_2O_3$	5	634	687	53	702	0.73	0.925
				10	639	695	56	709	0.98	
				15	643	699	56	716	1.01	
				20	648	705	57	720	0.98	

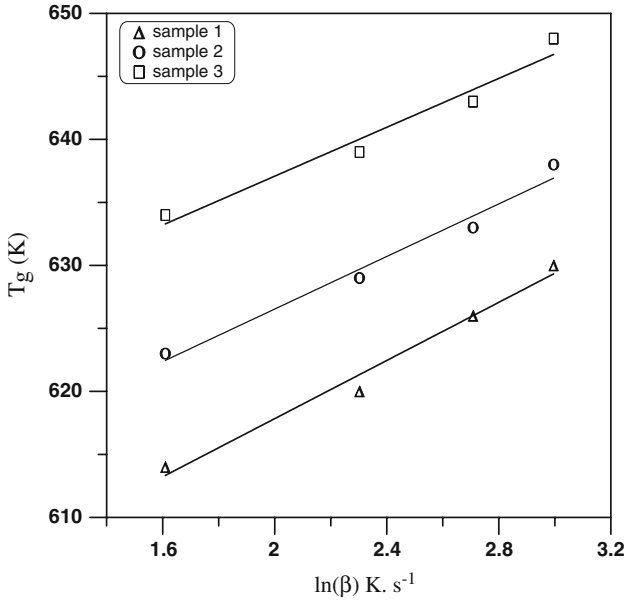

Fig. 2 Glass transition temperature T_g versus $\ln(\beta)$ in K min^{-1}

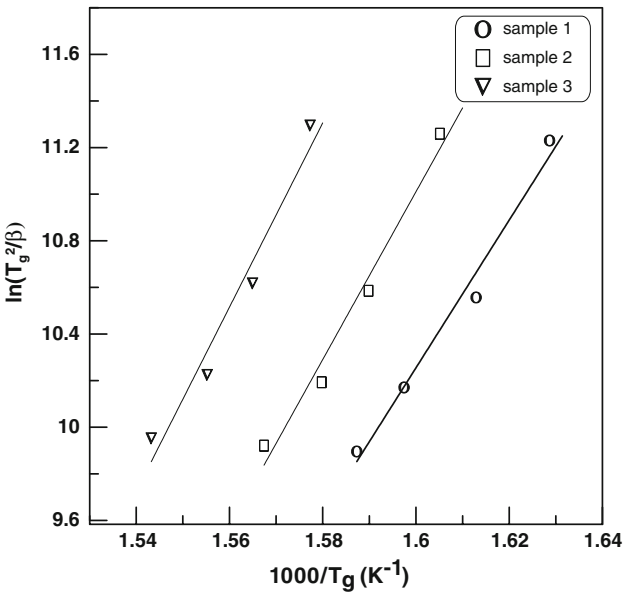

Fig. 3 Plot of $\ln(T_g^2/\beta)$ versus $1000/T_g$ of studied glasses

that the slope B in the Eq. 11 is related to the cooling rate of the melt (i.e., the lower the value of B the lower cooling rate of the melt). The physical significance of B seems to be related with the response of configurational changes within the glass transformation region.

The second approach concerns the use of the Kissinger's linear dependence [20] in the form:

$$\ln\left(\frac{\beta}{T_g^2}\right) = \frac{-E}{RT_g} + \text{constant} \tag{12}$$

In addition, a straight line between $\ln\left(\frac{\beta}{T_g^2}\right)$ and $\left(1/T_g\right)$, the slope of which yields a value of E and where the subscript g denotes magnitude values corresponding to T_g.

Given that the variation of $\ln\left(T_g^2\right)$ with β is negligibly small compared with the variation of $\ln(\beta)$, it is possible to write [20, 21]

$$\ln\beta = -\frac{E}{RT_g} + \text{constant} \tag{13}$$

The plots of $\ln\left(\beta/T_g^2\right)$ $\left(\text{in K}^{-1}\ \text{s}^{-1}\right)$ and $\ln(\beta)\left(\text{in K}^{-1}\ \text{s}^{-1}\right)$ vs. $10^3/T_g$ $\left(\text{in K}^{-1}\right)$ for the prepared glasses are shown in Figs. 3 and 4, respectively. Using the slopes of these plots, the

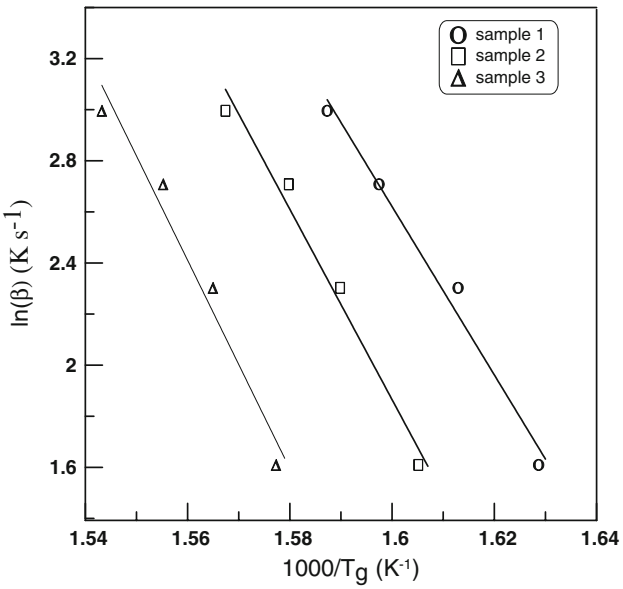

Fig. 4 Plot $\ln(\beta)$ versus $1000/T_g$ of studied glasses

activation energy values of the glass transition process are calculated for various glasses and are given in Table 2. This shows that one can use either of the Eqs. 12 and 13 for the

Table 2 A and B are constants for a given glass composition, activation energy for glasses transition E, and activation energy for crystallization E_G for prepared glasses

Sample name	$T_g = A + B\ln\beta$		E in (cal mol^{-1})		E_G in (cal mol^{-1})			<E_G> in cal mol^{-1}
	A	B	By Eq. 12	By Eq. 13	By Eq. 14	By Eq. 15	By Eq. 16	
Sample 1	594.76	11.5	63.17	65.55	84.34	87.08	85.71	85.71
Sample 2	605.67	10.43	71.64	74.15	75.76	78.5	77.15	77.14
Sample 3	617.7	9.7	78.61	81.21	72.87	75.62	74.23	74.24

evaluation of E. The glass transition activation energy, E, is the amount of energy absorbed by a group of atoms in the glassy region, which makes a jump from one metastable state to another possible. This means that E is involved in the molecular motions and rearrangements of atoms in the glass transition region. In the prepared glasses, the glass transition activation energy increased from 63.17 to 78.61 (in cal mol^{-1}) when TiO_2 content increased from 6 to 15 mol% see Table 2—(column 3) .

According of Kissinger [20], the peak crystallization temperature, T_P (in K), in terms of the heating rate β, can be expressed as

$$\ln\left(\frac{\beta}{T_P^2}\right) = -\left(\frac{E_G}{RT_P}\right) + \text{constant} \tag{14}$$

This equation is used to calculated the activation energy of crystallization by plotting $\ln\left(\beta/T_P^2\right)\left(\text{in K}^{-1}\,\text{s}^{-1}\right)$ vs. $10^3/T_P\left(\text{in K}^{-1}\right)$.

Also, E_G, can be calculated by the following equation:

$$\ln(\beta) = -\left(\frac{E_G}{RT_P}\right) + \text{constant} \tag{15}$$

The activation energy of crystallization can also be determined by an approximation method developed by Augis and Bennett [21]. The relation used by them is of the form:

$$\ln\left(\frac{\beta}{T_P}\right) = -\frac{E_G}{RT_P} + \ln K_0 \tag{16}$$

The activation energy of crystallization can be evaluated by this equation using the plots of $\ln(\beta/T_P)\left(\text{in K}^{-1}\,\text{s}^{-1}\right)$ vs. $10^3/T_P$. This method has an extra advantage in that the intercept of $\ln(\beta/T_P)$ vs. $10^3/T_P$, gives the value of pre-exponential factor K_0 (in s^{-1}) of Arrhenius equation.

The plots of $\ln\left(\beta/T_P^2\right)$, $\ln(\beta)$, and $\ln(\beta/T_P)$ vs. $10^3/T_P$ for prepared glasses are shown in Figs. 5, 6, and 7, respectively. Using the slopes of these plots, the activation energy of the crystallization process is calculated for the prepared glasses and is given in Table 2. It is clear from this table that the mean value of $\langle E_G \rangle$ decreased from 85.71 to 74.24 (in cal mol^{-1}) when TiO_2 content increased from 6 to 15 mol% in the prepared glasses. In order to identify

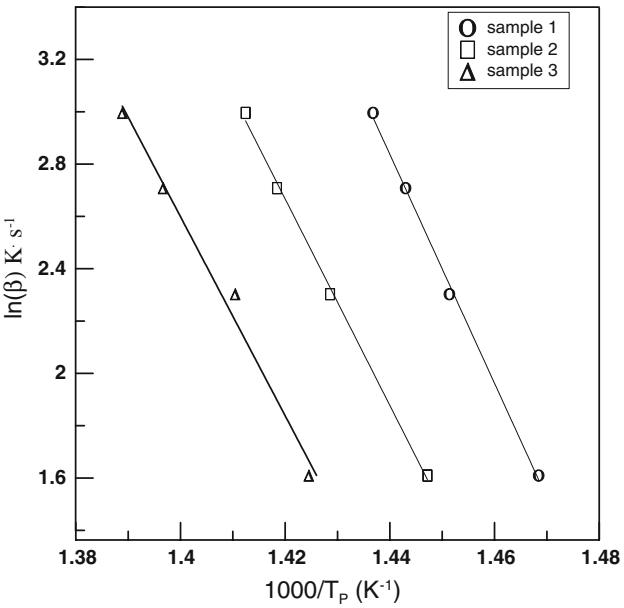

Fig. 6 Relation between $\ln(\beta)$ and $1000/T_P$ for prepared glasses

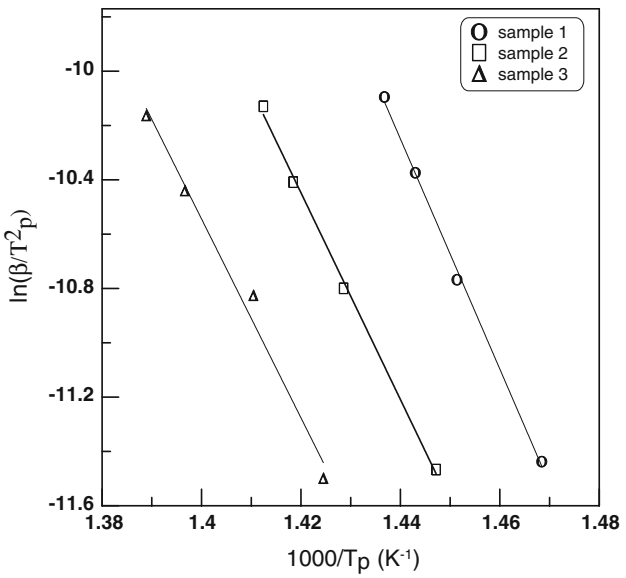

Fig. 5 Relation between $\ln(\beta/T_P^2)$ and $1000/T_P$ for prepared glasses

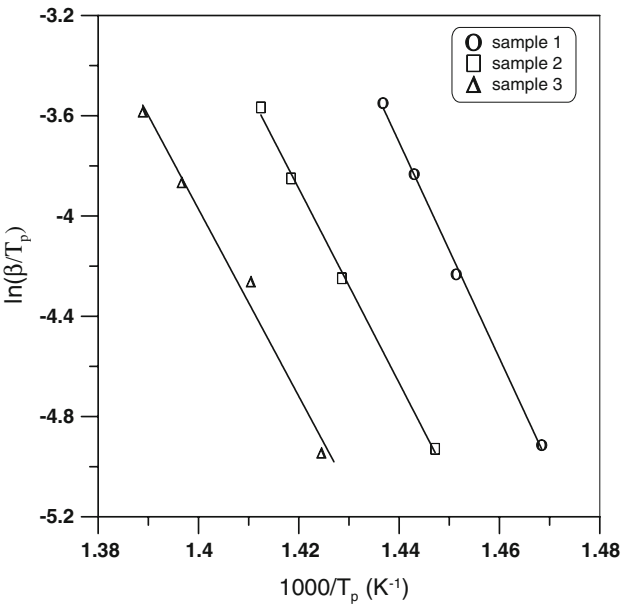

Fig. 7 Relation between $\ln(\beta/T_P)$ and $1000/T_P$ for prepared glasses

the possible phases that crystallize during the thermal treatment applied to the sample, Udovic et al. [22] had already reported on the synthesis of the crystalline phase $TiTe_3O_8$ in the TeO_2/TiO_2 glasses. Actually, the formation of those glasses with increasing, x, would change the coordination polyhedrons neither around Ti atom nor around Te atom but would result in the following alterations (a) the disappearance of the interchain Te–O–Te linkages which are weak since they involve the weak axial Te–O bonds $\approx$2.15 Å and the formation of stronger Te–O–Ti bridge (made of two relatively, strong bonds having 1.95 Å in length) replacing the just mentioned Te–O–Te. Therefore, in our opinion, the crystalline phase of prepared glass can be specified as $TiTe_3O_8$.

The area under the DTA curve is directly proportional to the total amount of amorphous crystallized. The ratio between the coordinates and the total area of the peak gives the corresponding crystallization rates, which make it is possible to plot the curves of the exothermal peaks (see Fig. 8a–c). It is observed that the $(dx/dt)_p$ as well as the heating rate values increase, a property which has been widely discussed in the literature [21].

Based on the E_G value it is possible to determine, through relationship (Eq. 10), the kinetic exponent, n, for

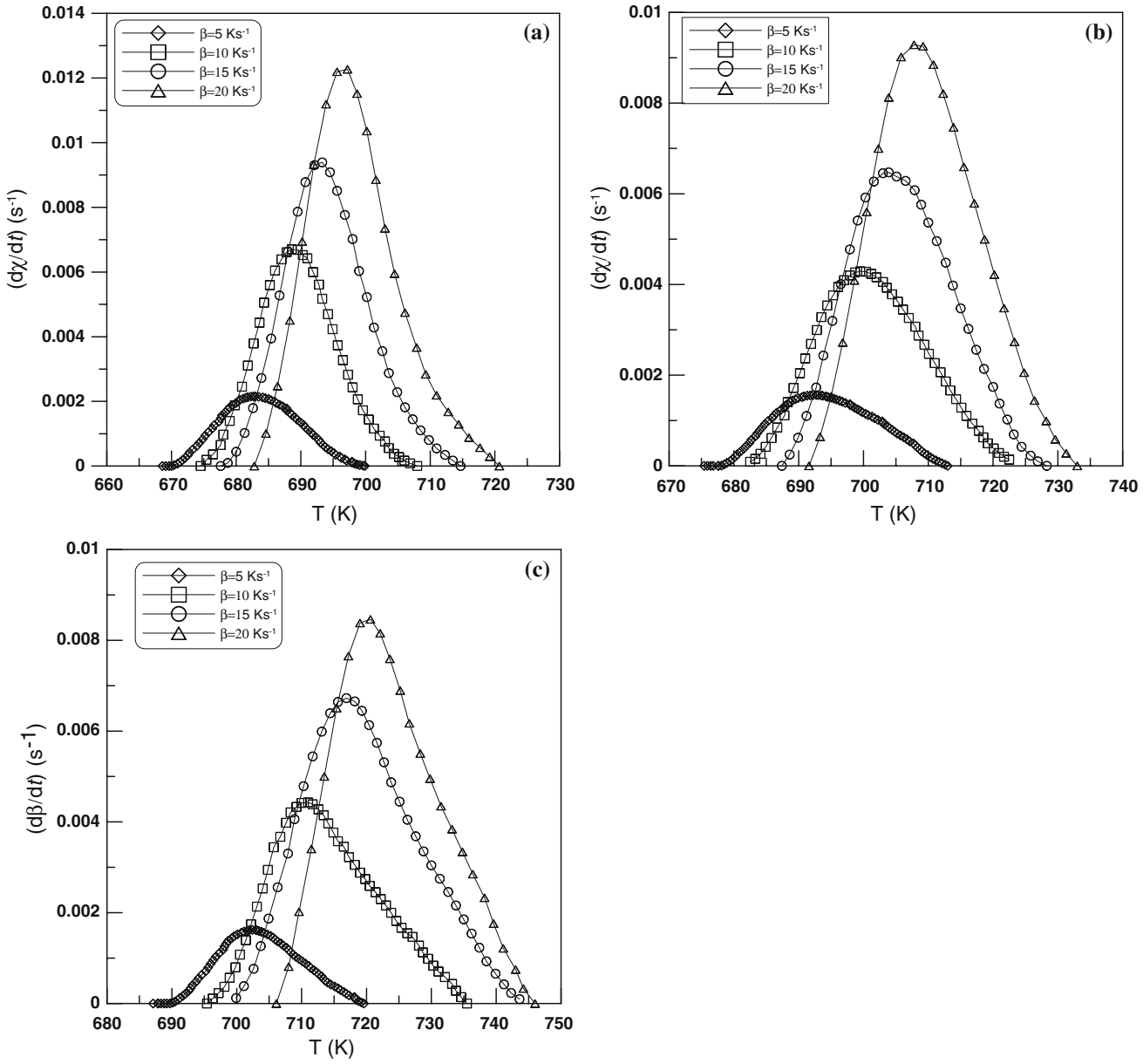

Fig. 8 **a** Crystallization rates versus temperatures of the exothermal peaks at different heating rates for sample 1, **b** crystallization rates versus temperatures of the exothermal peaks at different heating rates for sample 2, **c** crystallization rates versus temperatures of the exothermal peaks at different heating rates for sample 3 glass

each experimental heating rate for exothermic peak of crystallization, whose values are also given in Table 1; the mean value $\langle n \rangle$ changed from 1.07 to 0.925 with different compositions in our prepared glasses.

The graphical representation of the volume fraction crystallized shows the typical sigmoid curve as a function of temperature for different heating rates for crystallization peak of prepared glasses (see Fig. 9a–c).

The value of Avrami exponent can be evaluated from the relation between $\ln[-\ln(1-\chi)]$ and $\ln(\beta)$ at constant temperature and can be written as [23, 24],

$$\frac{d[\ln[-\ln(1-\chi)]]}{d\ln(\beta)} = -n_a \tag{17}$$

where, n_a is an integer depending on the morphology of the crystal growth. Figure 10 shows the plots of $\ln[-\ln(1-\chi)]$

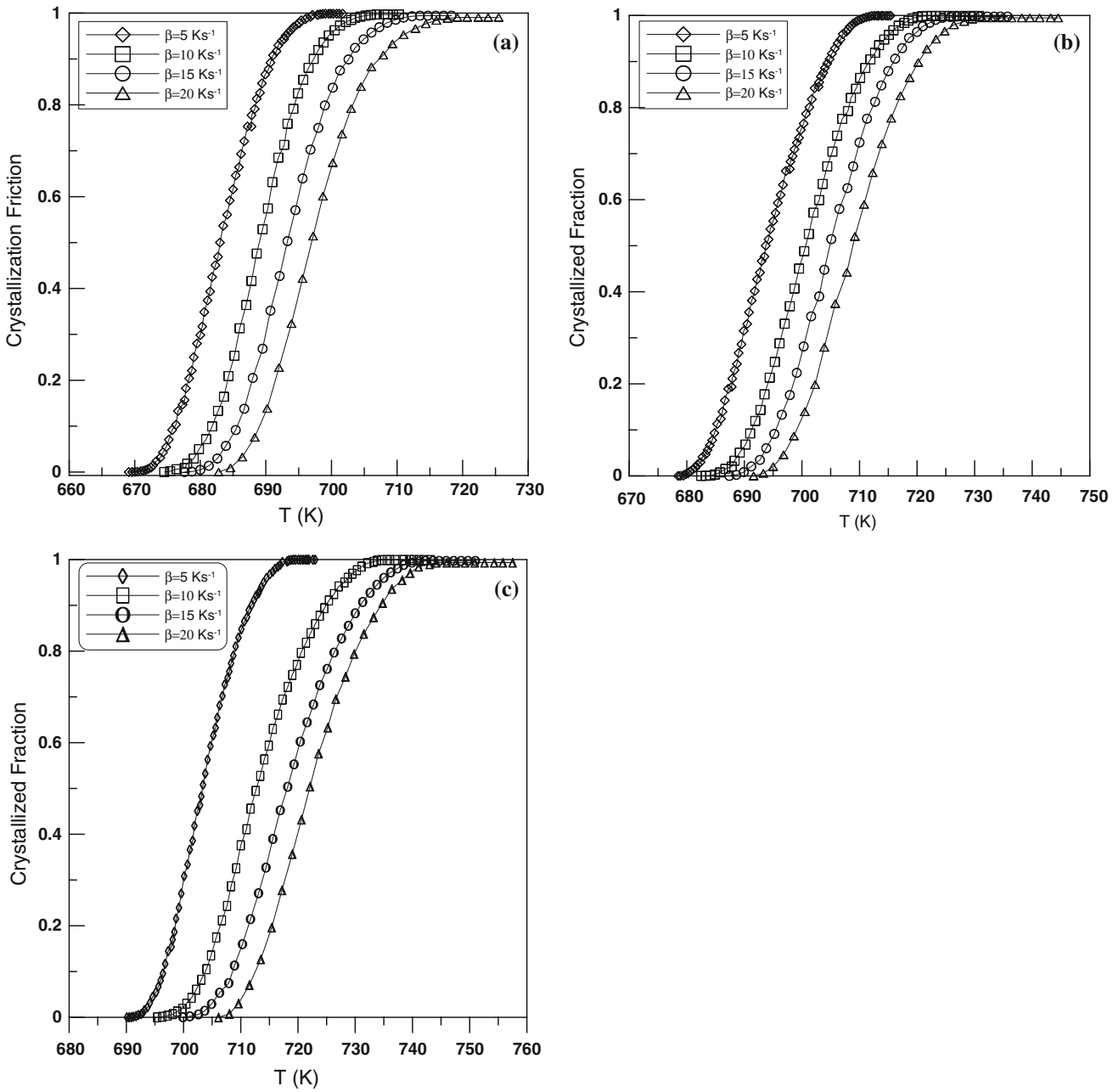

Fig. 9 **a** Crystallized fraction as a function of temperature of exothermal peak at different heating rates for sample 1, **b** crystallized fraction as a function of temperature of exothermal peak at different heating rates for sample 2, **c** crystallized fraction as a function of temperature of exothermal peak at different heating rates for sample 3

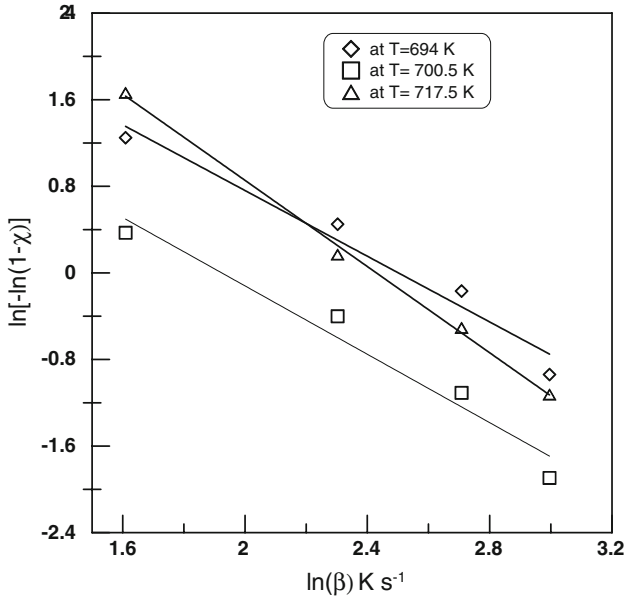

Fig. 10 Relation between $\ln[-\ln(1-\chi)]$ versus $\ln(\beta)$ for studied glasses

and $\ln(\beta)$ at different temperatures. From the slopes of this relation, the values of n_a are found to be 1.51, 1.58, and 1.99 at 694, 700.5 and 717.5 K, respectively. The calculated value of the order of the crystallization reaction, n, indicates that (TeO_2–TiO_2–As_2O_3) glasses crystallize two-dimensionally.

Conclusion

The kinetic parameters, activation energy of the glass transition, activation energy for crystallization process, kinetic exponent, n, and exponential factor for TeO_2/TiO_2 glasses with small additive As_2O_3 oxide have been deduced depending on the heating rate. The changes of these parameters can be traced out by continuous variation in the glasses composition. It is found that the T_g value increases with increasing concentration of TiO_2 content. The glass transition activation energy increased from 63.17 to 78.61 (in cal mol^{-1}) when TiO_2 content increased from 6 to 15 mol%. The mean value of $\langle E_G \rangle$ decreased from 85.71 to 74.24 (in cal mol^{-1}) when TiO_2 content increased from 6 to 15 mol% in the prepared glasses.

References

1. Vogel EM, Weber MJ, Krol DM (1994) Phys Chem Glass 32:231
2. El Mallawany R (2002) Handbook of tellurite glasses, physical properties & data. CRC Press, Boca Raton, FL
3. Kim HG, Komatsu T, Shioya K, Matusia K, Tanka K, Hirao K (1996) J Non-Cryst Solids 208:303
4. Yousef E, Hotzel M, Russel C (2004) J Non-Cryst Solids 342:82
5. Lines ME (1990) Phys Rev B 41:3383
6. Berthereau A, Fargin E, Villezusanne A, Olazcuaga R, Flem GL, Deucasse L (1996) J Solid State Chem 126:143
7. Noguera O, Smirnov M, Mirgrorodsky AP, Merle-Mejean T, Thomas P, Champarnaud Mesjard JC (2004) J Non-Cryst Solids 345346:734
8. Noguera O, Merle-Mejean T, Mirgrorodsky AP, Thomas P, Champarnaud Mesjard JC (2004) J Phys Chem Solids 65:981
9. Durga DK, Yadagiri Reddy P, Veeraiah N (2002) J Luminescence 99:53
10. Colton A, Wilkinson G, Murillo CA, Bochmann M (1999) Advanced inorganic chemistry. John Wiley & Sons, New York, NY
11. Chung CH, Meckenzie JD (1980) J Non-Cryst Solids 42:357
12. Avrami M (1941) J Chem Phys 9:117
13. Khan SA, Zulfequar M, Husain M (2002) J Phys Chem Solids 123:463
14. Kaap SO, Juhasz C (1985) J Chem Soc, Faraday Trans 2(81):811
15. Vazquez J, Wagner G, Villares P, Jimenez Garay R (1996) Acta Mater 44:4807
16. Yinnon H, Uhlmann DR (1983) J Non-Cryst Solids 54:253
17. Vazquez J, Garcia D, Barreda G, Lopez Alemany PL, Villares P, Jimenez Geray R (2004) J Non-Cryst Solids 345&346:142
18. Shaaban ER (2006) Physica B 373:211
19. Losocka M (1976) Mater Sci Eng 23:173
20. Kissinger HE (1957) Anal Chem 29:1702
21. Augis JA, Bennett JE (1978) J Anal 13:283
22. Udovic M, Thomas P, Mirgorodsky A, Durand O, Soulis M, Masson O, Merle-Mejean T, Champarnaud-Mesjard JC (2006) J Non-Cryst Solids 179:3252
23. Grant FA (1959) Rev Mod Phys 31:646
24. Avrami M (1940) J Phys Chem 7:212